

Mullitisation behaviour of calcined clay–alumina mixtures

V. Viswabaskaran^{a,1}, F.D. Gnanam^{a,2}, M. Balasubramanian^{b,*}

^aCentre for Ceramic Technology, Anna University, Chennai 600 025, India

^bComposite Technology Centre and Department of Metallurgical Engineering, Indian Institute of Technology, Chennai 600 036, India

Received 23 May 2002; received in revised form 12 June 2002; accepted 20 August 2002

Abstract

The mullitisation behavior of three south Indian calcined clays with three different alumina sources has been studied. The calcined clays were ground and then mixed with different alumina sources such as reactive alumina, gibbsite and boehmite. Rectangular bars were prepared and sintered at 1600 °C/3 h. The X-ray diffraction and microstructural analysis were carried out to understand the mullitisation behavior. Thermogravimetric and differential thermal analyses of the powders were also carried out. The physical and mechanical properties were measured and discussed. The calcined clay (meta kaolin) derived samples show better strength and density than the uncalcined clay derived sample. The microstructure also shows a higher aspect ratio of mullite crystals. Among the three clay combinations, the calcined Neyveli clay and fine reactive alumina mixture was found to exhibit a better mullitisation behavior compared to other combinations.

© 2003 Elsevier Science Ltd and Techna S.r.l. All rights reserved.

Keywords: A. Calcination; A. Sintering; C. Mechanical properties; D. Clays; D. Mullite

1. Introduction

Mullite is a promising material for both conventional and advanced (including electrical and structural) ceramic applications due to low density (3.17 g cm^{-3}), low thermal conductivity ($k=2.0 \text{ Wm}^{-1} \text{ K}^{-1}$), low thermal expansion coefficient ($20/200 \text{ °C}=4\times 10^{-6} \text{ K}^{-1}$), low dielectric constant ($\epsilon=6.5$ at 1 MHz) and excellent mechanical properties at high temperature [1,2]. Though extensive efforts have been made to synthesis mullite powders [3–5] and to prepare dense sintered bodies, these methods involve very high cost starting materials and processing techniques that made them not suitable for large scale commercial production [6]. Cheaper alternative ways of synthesis using raw materials like kaolinite, sillimanite, alumina, gibbsite and boehmite have been frequent subject of research [7–9].

It is well known that kaolinite will undergo a series of reactions during the early stages of heating [10]. Studies on the kaolinite reaction series based on differential thermal analysis (DTA) have revealed that [11] the endothermic peak in the temperature range 500–600 °C corresponds to dehydration and the three exothermic peaks occurring at around 980, 1250 and beyond 1300 °C are due to the formation of spinel, 3:2 mullite and amorphous silica respectively. The kaolinite–meta-kaolin transformation proceeds very slowly and meta-kaolin has an extreme defect structure; about 20 vol.% of the metakaolin consists of lattice vacancies produced by the temperature-induced water release [12]. This may be the reason for lower physical and mechanical properties of uncalcined kaolinite and alumina mixtures as reported in our earlier studies [13,14]. According to Charkborthy [15] and Chaudhri [16] calcination of clays at 1400 °C leads to the formation of mullite and silica. In the present study the clays from three different locations [14] in southern part of India were calcined at 1400 °C for 3 h for completion of all the reactions. Then the calcined clays were wet ball milled for 5 h using alumina grinding media. This calcined clay powder was mixed with appropriate amount of either reactive alumina or gibbsite or boehmite to prepare stoichiometric

* Corresponding author. Tel.: +91-44-257-8609/257-9609; fax: +91-44-257-0039/257-0545.

E-mail addresses: mbala@iitm.ac.in (M. Balasubramanian), zeramist@yahoo.co.in (V. Viswabaskaran), fdgnanam@yahoo.com (F.D. Gnanam).

¹ Tel.: +91-44-442-2170.

² Tel.: +91-44-445-1722; fax: +1-91-44-23-52870.

mullite. Thermo gravimetric analysis (TGA) and differential thermal analysis (DTA) were carried out to understand the reactions. X-ray diffraction (XRD) and scanning electron microscope (SEM) were used to find the final mullitisation of each sample. The physical properties like density and flexural strength were measured and compared.

2. Experimental

The clays from southern region of India (Neyveli, Panruti and Udayarpalayam) were washed as per standard

procedure discussed elsewhere [17] and calcined to a temperature of 1400 °C for 3 h. The calcined clays were milled for a mean grain size of 2.0 µm. Reactive alumina from Alcoa (SG9000, and mean grain size 0.7 µm) and gibbsite from Indal (mean grain size 2 µm) and boehmite prepared from alkoxide route [18] were used as the alumina sources. The chemical composition of the starting materials is listed in Table 1. As per the stoichiometric composition [19], the materials were weighed and wet milled for half an hour in a planetary mill using alumina balls. The slurries were dried at 100 °C for 72 h [7].

The particle size distribution analysis of the starting raw materials was carried out using Shimadzu laser

Table 1
Chemical analysis of raw materials (wt.%)

Elements	Panruti clay	Neyveli clay	Udayarpalayam clay	Reactive alumina	Gibbsite
LOI	13.42	16.00	13.70	–	32.77
SiO ₂	49.06	43.26	52.09	0.01	0.18
Al ₂ O ₃	33.07	36.11	29.92	99.85	64.35
Fe ₂ O ₃	2.22	1.06	1.83	0.02	0.23
TiO ₂	1.20	1.59	0.78	–	–
CaO	0.51	0.37	1.03	0.01	2.22
MgO	0.23	1.40	0.48	–	0.02
Na ₂ O	0.19	0.11	0.16	0.08	0.25
K ₂ O	0.11	0.10	–	–	–

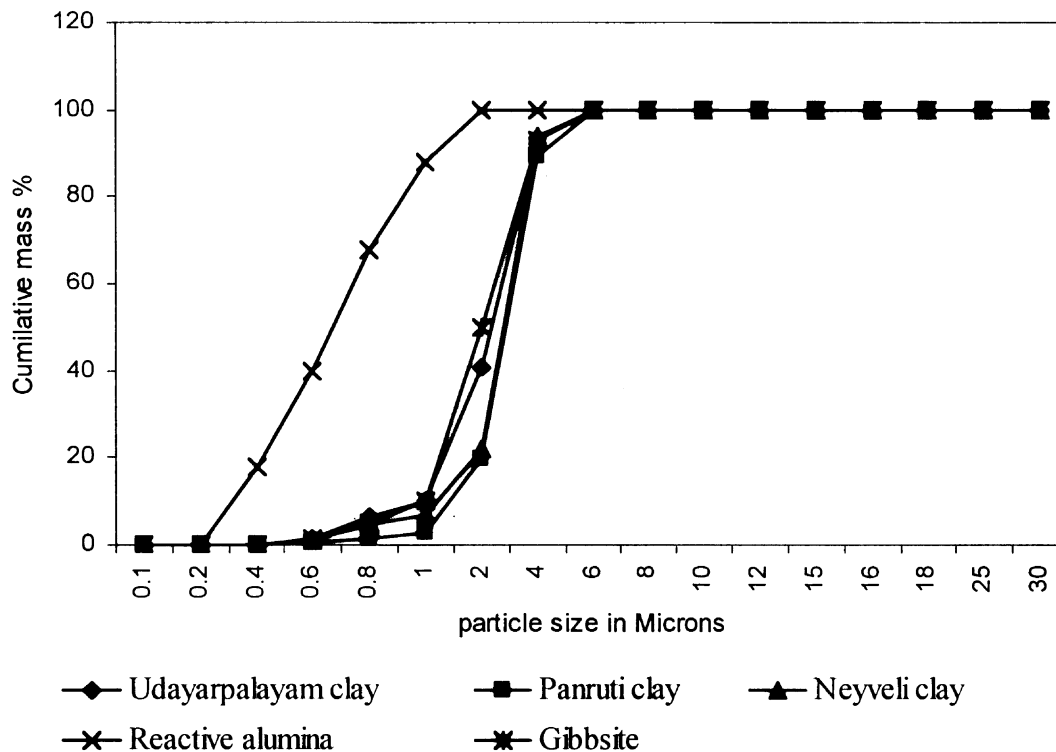


Fig. 1. Particle size distribution of raw materials.

particle size analyzer (SALD 1100). Powders were characterised by DTA and TGA using NETZSCH STA 409PC with α -alumina as the reference material at a heating rate of $5\text{ }^{\circ}\text{C min}^{-1}$ in air. The powder samples of -200 ASTM mesh size were dried at $110\text{ }^{\circ}\text{C}$ for 2 h before thermal analysis. The powders were pressed into rectangular bars using uniaxial pressing and were sintered in an electric furnace at a heating rate of $5\text{ }^{\circ}\text{C min}^{-1}$ in air to $1600\text{ }^{\circ}\text{C}$ and soaked for 3 h before furnace cooling. The pure clay bars prepared from the above sources were also sintered along with the above specimens to study the characteristics of cristobalite formation in the absence of alumina. The phases present in sintered samples were identified by XRD using Siemens D-500 powder diffractometer using $\text{Cu } K_{\alpha}$ radiation at a scan rate of $2^{\circ}\text{ min}^{-1}$. For XRD analysis, the compacts were heated at the same rate as the DTA

analysis and then powdered and used. The bulk density of the pellets was determined using Archimedes principle. Modulus of rupture (MOR) was determined on rectangular samples sintered at $1600\text{ }^{\circ}\text{C}/3\text{ h}$ using universal testing machine (Zwick 1445). The samples were polished and thermally etched for 1.0 h at $1500\text{ }^{\circ}\text{C}$ and subsequently examined under scanning electron microscope (SEM) using Cambridge Instruments-5526 scanning electron microscope.

3. Results and discussion

The results of chemical analysis of the different raw materials used for this investigation are presented in Table 1. The particle size distribution of ground clay materials, reactive alumina and gibbsite are given in

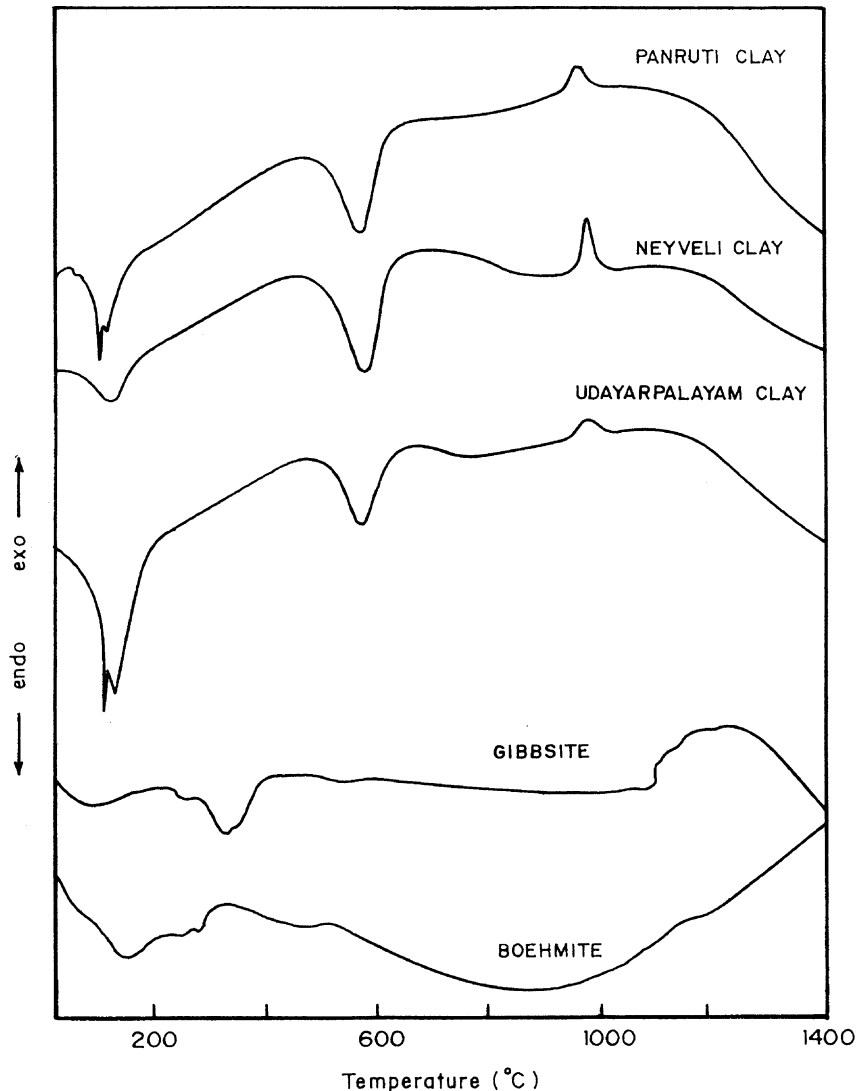


Fig. 2. Differential thermal analysis of raw materials.

Fig. 1. The mean particle size of the reactive alumina is 0.7 μm and gibbsite is 2 μm . The particle size of the milled clays is kept between 2 and 3 μm .

The differential thermal analyses for starting raw materials are shown in Fig. 2. The Neyveli and Panruti clays indicate the presence of highly crystalline kaolinite showing the characteristic peaks in their usual positions [16]. The results of clay samples reveal an endothermic peak at around 110 $^{\circ}\text{C}$ from vaporization of absorbed water and at 500–600 $^{\circ}\text{C}$ is due to loss of structural water. The prominent exotherm at around 980 $^{\circ}\text{C}$ corresponds to the formation of 2:1 mullite and spinel from metakaolin. A much smaller exothermic peak is found at around 1200–1250 $^{\circ}\text{C}$ (observed in derivative curve) associated with 3:2 mullite formation [9]. The DTA curve for boehmite shows three successive endothermic peaks up to 460 $^{\circ}\text{C}$ and an exothermic peak at 1170 $^{\circ}\text{C}$. The first two endothermic peaks at 160 and 255 $^{\circ}\text{C}$ are due to the loss of absorbed water and structural water respectively and the third endothermic peak is due to transformation of boehmite into γ -alumina. The exothermic peak is due to transformation of γ -alumina to α -alumina [18].

Thermogravimetric analyses for starting materials are shown in Fig. 3. The clay samples lose their weight in

two temperature regions. The first loss in weight (around 110 $^{\circ}\text{C}$) may be attributed to the loss of surface water. The second loss in weight around 545–535 $^{\circ}\text{C}$ is due to the loss of structural water (OH groups attached to Al and Si) [22]. Both these changes in TGA are indicated by endothermic changes in DTA curves. The absence of any further change in weight at higher temperatures, after the dehydroxylation is complete, confirms that the exothermic change at around 980 $^{\circ}\text{C}$ in DTA of the specimens is due to phase change only. The TGA results of gibbsite show that the weight losses at around 350 and 500 $^{\circ}\text{C}$ are due to dehydration of structural water. The TGA curve of boehmite exhibits weight loss continuously up to 460 $^{\circ}\text{C}$ and thereafter no significant weight loss has been observed. The TGA result of boehmite shows that the total water loss has been very high ($\approx 41\%$).

The thermogravimetric analysis results of the calcined clays with different alumina sources are given in Fig. 4. The weight loss till 1400 $^{\circ}\text{C}$ is almost zero for the calcined clays containing reactive alumina, except the Udayarpalayam clay sample, the maximum weight loss was noted up to 0.9% and this may be due to the physically absorbed moisture. But for the samples contain-

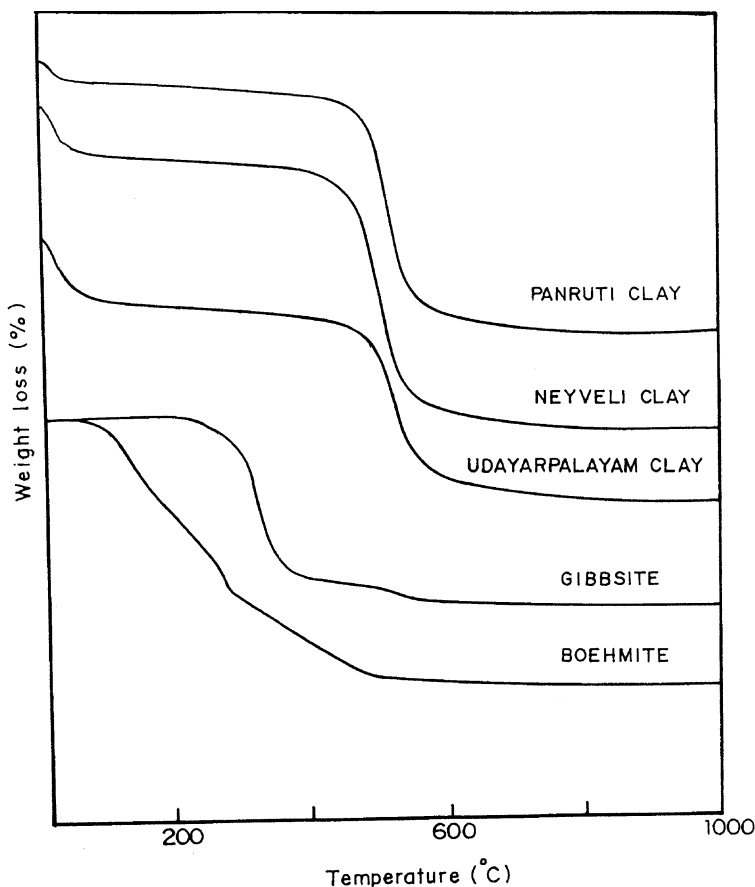


Fig. 3. Thermo gravimetric analysis of raw materials.

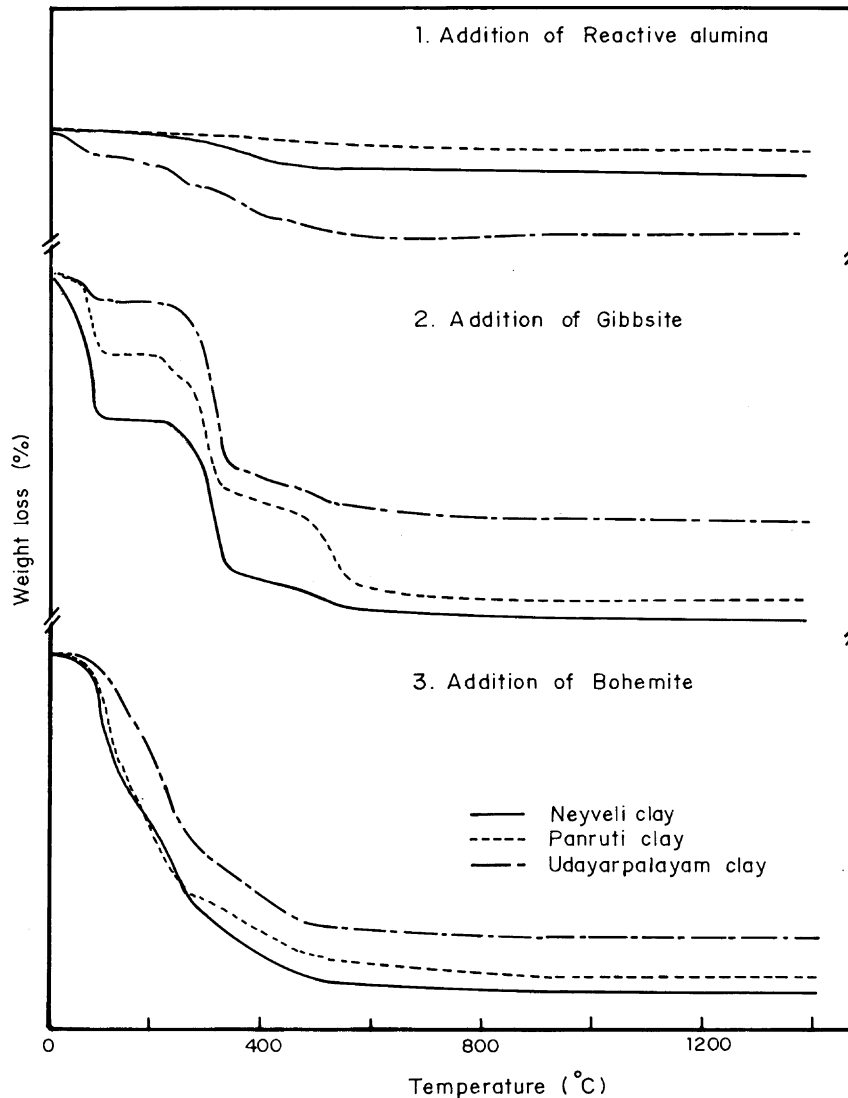


Fig. 4. Thermo gravimetric analysis of calcined clays with alumina sources.

ing gibbsite, the TGA results show that the weight losses occur at around 300 and 500 °C are due to dehydration of gibbsite. The thermogravimetric analysis for boehmite containing samples shows that the continuous weight loss occurred up to around 475 °C is due to loss of chemically combined water from the boehmite and transformation into γ -alumina.

The differential thermal analysis results for calcined clays with different alumina sources are shown in Fig. 5. The clay–reactive alumina mixture does not show any significant change up to 1150–1200 °C. Around 1200 °C there is a weak exothermic peak (observed in the derivative curve) that confirms the reaction between the clay and alumina. The DTA result for clay–gibbsite mixture shows that the sharp endothermic peak at 300 °C and small endothermic peaks at 250 and 500 °C are due to

dehydration of structural water present in gibbsite. The small exothermic peaks are observed at around 600 and 900 °C. The later event is due to the acceleration of mullite growth by liquid formation or by the reaction of spinel phase with excess silica [11]. All the three clay samples show similar peaks with respect to corresponding temperature. The boehmite containing samples show small endothermic peak at around 460 °C due to the conversion of boehmite to γ -alumina [18]. Another small exothermic peak is observed between 1150 and 1200 °C (observed in the derivative curve) due to the reaction of alumina and silica phase present in the clay matrix. The DTA results reveal that the reaction between metakaolin and alumina starts at lower temperature in the boehmite mixtures because of very fine alumina (boehmite) particles.

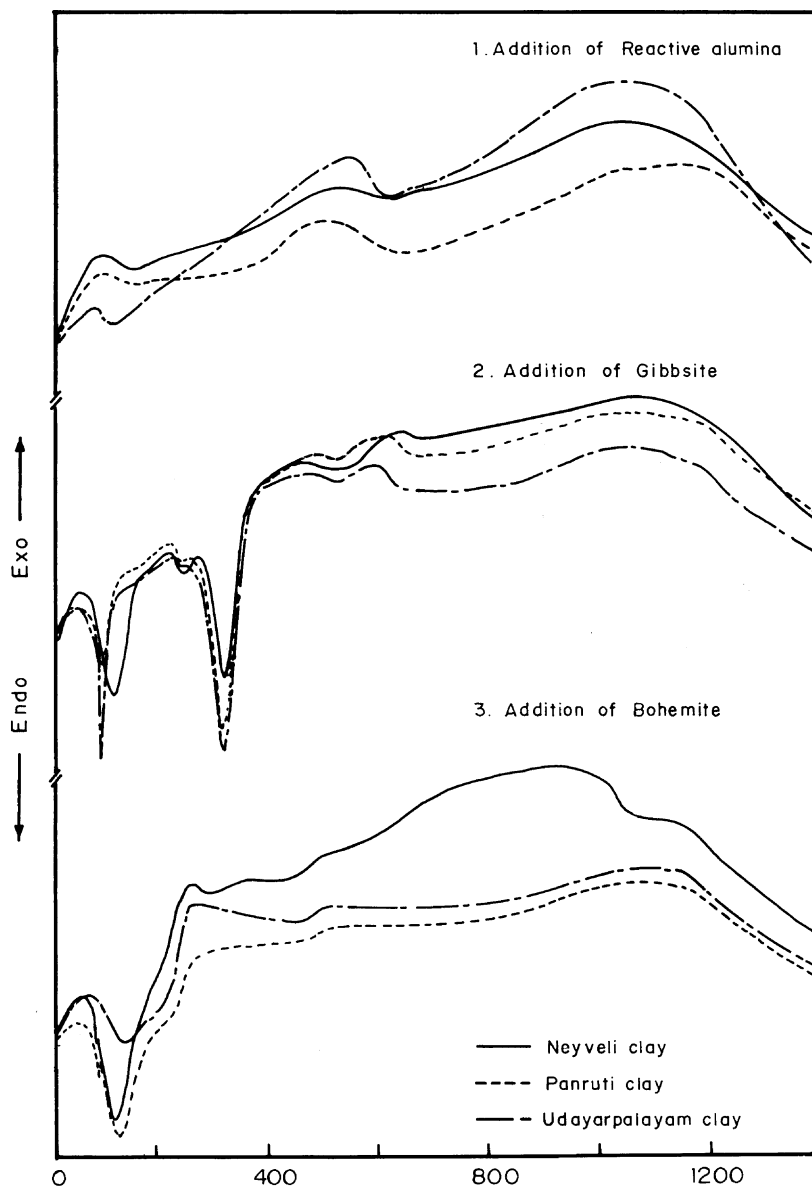


Fig. 5. Differential thermal analysis of calcined clays with alumina sources.

XRD patterns for clay–reactive alumina, gibbsite and boehmite are given in Figs. 6–8. Clay heated to a temperature above 1000 °C is converted into mullite and cristobalite [12], while the boehmite has to thermally transform to α -alumina through γ -alumina. The XRD results confirmed that all the samples have been fully converted into mullite. The reaction of α -alumina with liquid silicate to form mullite was extensive at 1500 °C [9], extremely fast at 1600 °C and 37 min soaking has been enough to complete the reaction [20]. The XRD results show that there is no evidence for the presence of cristobalite and α -alumina phase in any of the three clay

samples. This confirms that the reaction between alumina and liquid silicate from clay at 1600 °C is completed.

The micrographs of the sintered samples of calcined clays and reactive alumina mixtures are shown in Fig. 9. The microstructure shows a bimodal grain structure [7] of larger elongated primary mullite grains and smaller equiaxed secondary mullite grains. The Neyveli clay shows perfect primary and secondary rhombohedral shaped crystals. Panruti clay microstructures show more primary mullite crystals with sharp edges whereas in Udayarpalayam clay, the secondary mullite crystals are dominating with irregular morphology. The micro-

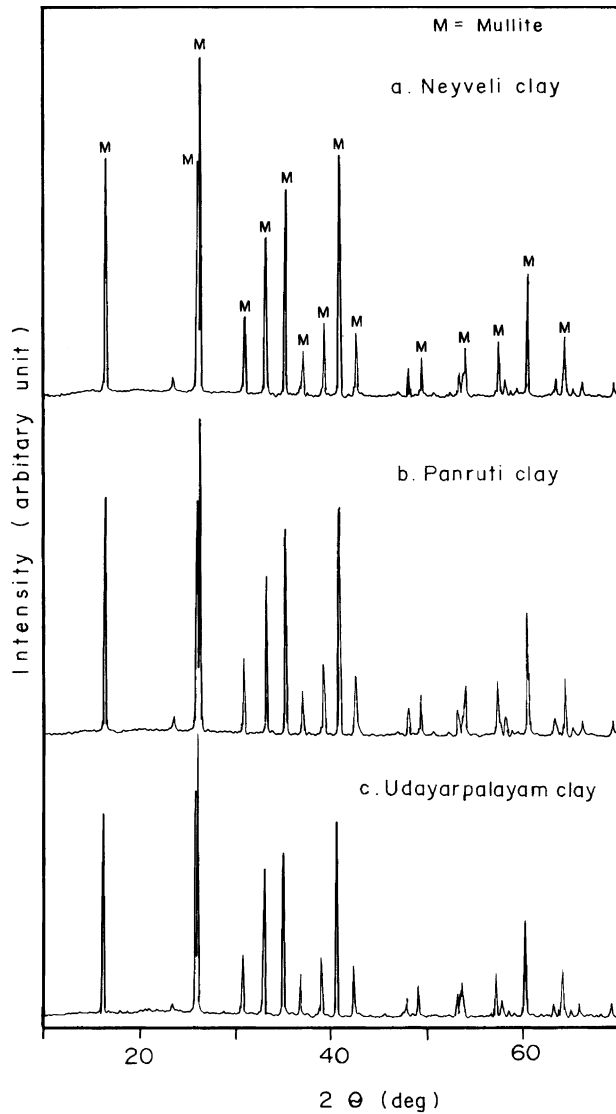


Fig. 6. XRD patterns of clay-reactive alumina samples sintered at 1600 °C for 3 h.

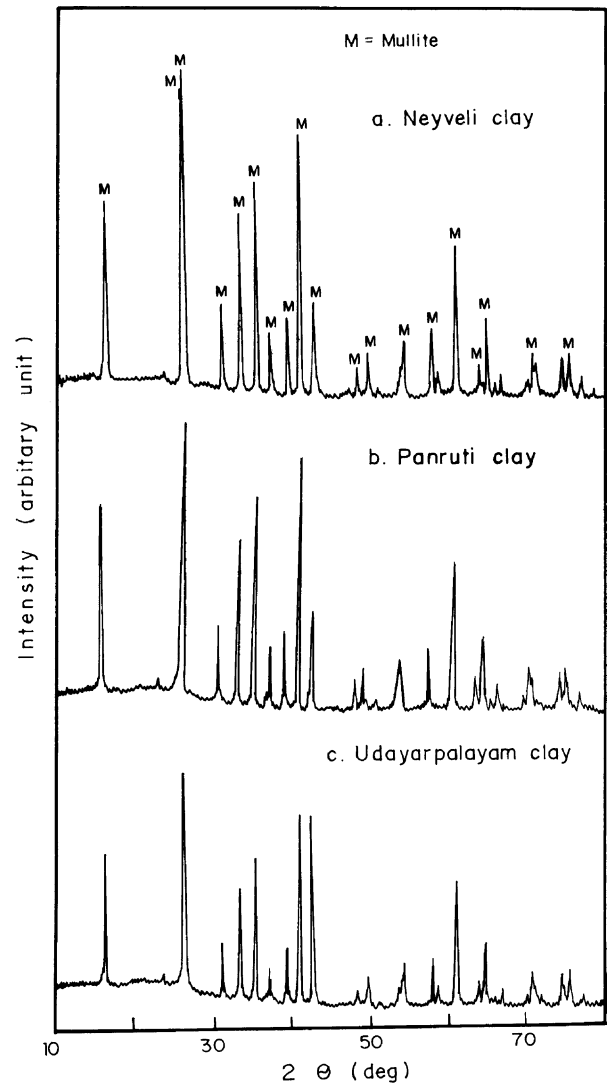


Fig. 7. XRD patterns of clay-gibbsite samples sintered at 1600 °C for 3 h.

Table 2
Physical properties of calcined clays with alumina additives (1600 °C/3 h)

Samples	Porosity (%)	Bulk density (g cm ⁻³)	MOR (MPa)
Neyveli clay + reactive alumina	4.99	2.79	91
Neyveli clay + gibbsite	4.41	2.67	91
Neyveli clay + boehmite	4.23	2.57	38
Panruti clay + reactive alumina	5.03	2.76	123
Panruti clay + gibbsite	4.33	2.70	99
Panruti clay + boehmite	6.33	2.58	29
Udayarpalayam clay + reactive alumina	5.87	2.81	135
Udayarpalayam clay + gibbsite	3.45	2.83	90
Udayarpalayam clay + boehmite	2.93	2.69	37

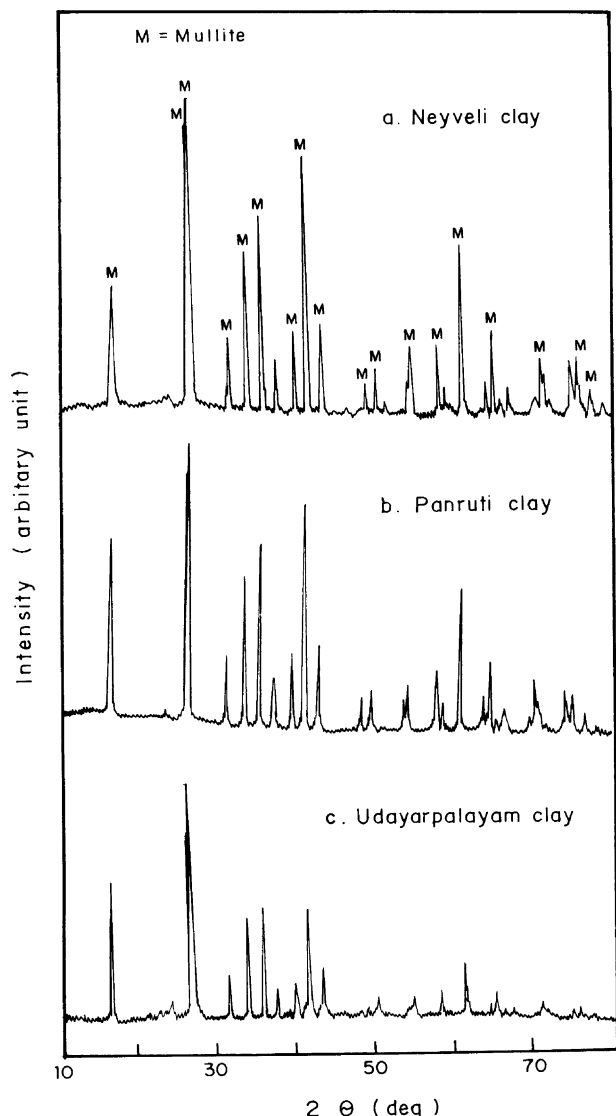


Fig. 8. XRD patterns of clay-boehmite samples sintered at 1600 °C for 3 h.

structures of the gibbsite containing clay samples show similar bimodal morphology as that of reactive alumina samples (Fig. 10). The Neyveli clay shows the presence of maximum amount of primary mullite crystals with high aspect ratio and sharp edges. The microstructure of Panruti clay shows that the aspect ratio is relatively smaller for the primary mullite crystals. The Udayarpalayam clay yields imperfect large mullite crystals. Few small grains are also observed in the structure due to impurities. The SEM micrographs of clay-boehmite samples (Fig. 11) reveal that the Neyveli clay-boehmite exhibits perfect rhombohedral crystals due to pure nature of clay and boehmite. The mullite crystals were bimodal in size, in the range of 1–2 μm for secondary crystals and 4–6 μm for primary mullite crystals. All the clay samples show very

distinctive rhombohedral shaped crystals. In Panruti and Udayarpalayam clays, maximum quantity of secondary mullite with few primary mullite crystals is observed.

From the microstructural analysis, the bimodal morphology is observed in all the experimental samples. In all the cases, the larger primary mullite crystals are well defined. The size of the primary mullite crystals is slightly larger in the boehmite containing samples. The quantity of primary mullite is high in reactive alumina mixtures. In the case of gibbsite mixtures, secondary mullite is dominating in quantity. According to the $\text{Al}_2\text{O}_3\text{-SiO}_2$ [21] system at temperatures higher than 1595 °C the process of dissolution of mullite in the liquid phase starts, and in the case of gibbsite, the temperature is still lower due to higher amount of impurities. The existence of this eutectic liquid, at temperatures around 1595 °C, will enhance the formation secondary mullite [7]. This is may be the reason for the gibbsite samples showing more equiaxed secondary mullite.

The bulk density and strength of the samples sintered at 1600 °C for 3 h are shown in Table 2. The maximum density (2.79 g cm^{-3}) has been observed for Neyveli clay-reactive alumina mixture and the maximum strength (135 MPa) have been obtained for Udayarpalayam clay and alumina mixture. The reaction bonded mullite shows that the physical properties depend primarily on the clay sources than the alumina sources. Due to the higher water loss ($\approx 41\%$) in boehmite, the boehmite containing samples have high porosity and exhibit poor mechanical properties.

The bulk density is maximum for the mullite obtained from calcined Neyveli clay and reactive alumina. This value is approximately 25% higher than that for the mullite obtained from uncalcined Neyveli clay and reactive alumina reported earlier [14]. The same trend was noted for all the clay and alumina sources. The kaolinite-metakaolin transformation proceeds very slowly, and metakaolin has an extreme defect structure: about 20 vol.% of the metakaolin consists of lattice vacancies produced by the temperature-induced water release [12]. These vacancies may not be completely removed in the mullite obtained from green clay-reactive alumina, results in lower density and flexural strength. Additionally in the sintering, volatile materials going out from the uncalcined clay, produces porosity. This porosity may not be completely eliminated during the sintering process. In the case of calcined clay, due to the high temperature calcinations and intensive size reduction, the calcined clay is free from porosity generated by volatile materials and yields dense and high flexural strength mullite. The calcined clays also yield more perfect mullite crystals than the uncalcined clays. This is another important

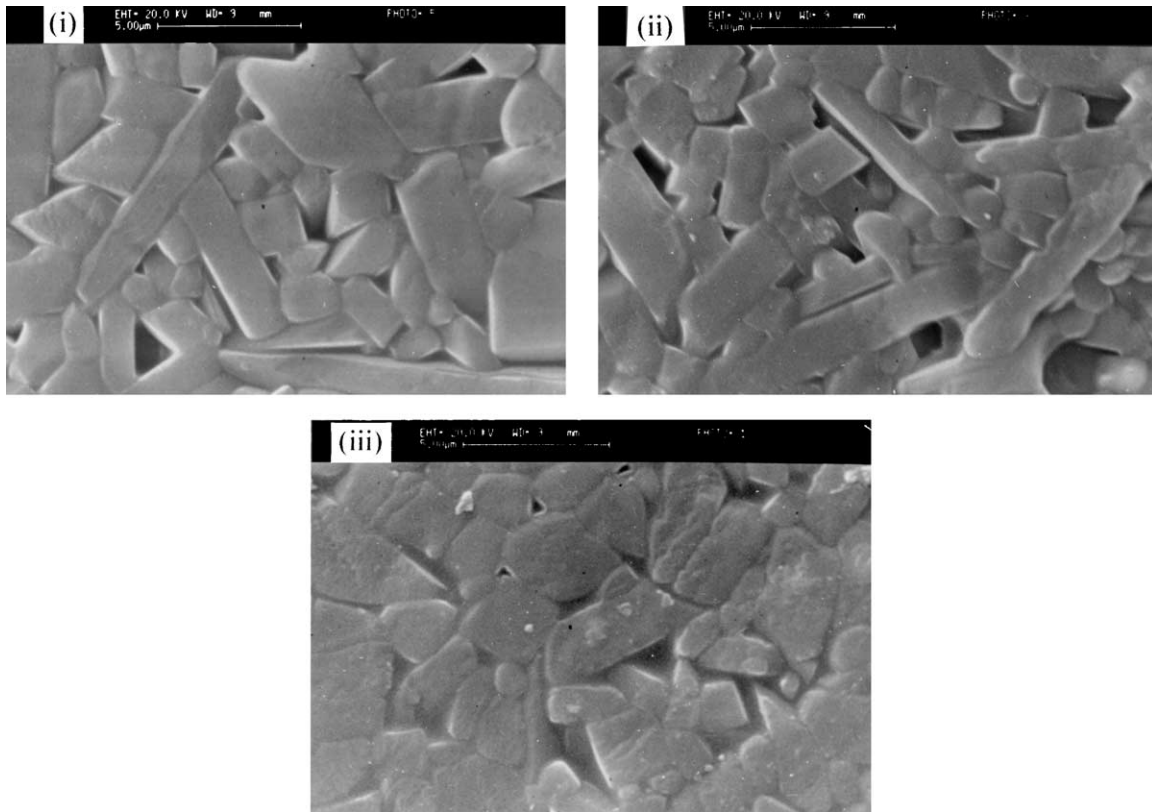


Fig. 9. Microstructures of calcined clays–reactive alumina sintered at 1600 °C for 3 h: (i) Neyveli clay, (ii) Panruti clay, (iii) Udayarpalayam clay.

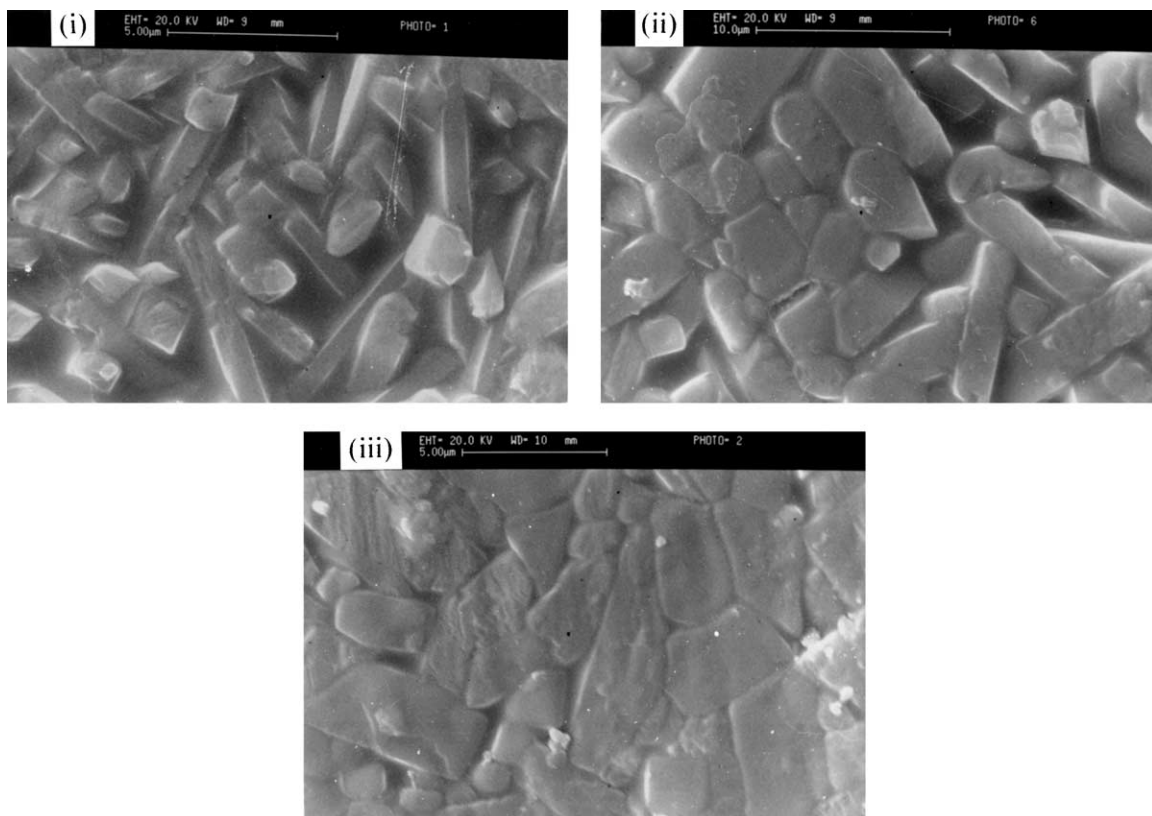


Fig. 10. Microstructures of calcined clays–gibbsite sintered at 1600 °C for 3 h: (i) Neyveli clay, (ii) Panruti clay, (iii) Udayarpalayam clay.

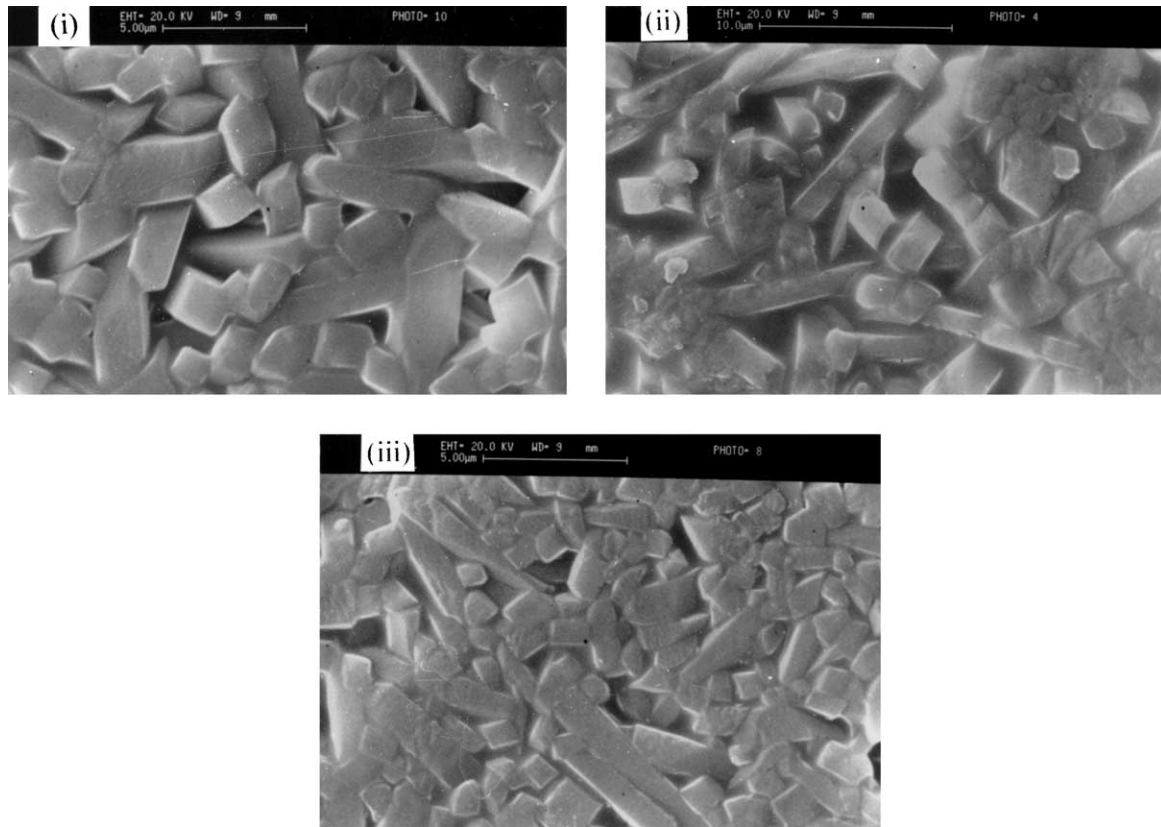


Fig. 11. Microstructures of calcined clays-boehmite sintered at 1600 °C for 3 h. (i) Neyveli clay, (ii) Panruti clay, (iii) Udayarpalayam clay.

reason, why the calcined clays-alumina yields better physical properties.

4. Conclusions

The following conclusions are drawn from the results of the present investigation.

1. The mullite formed from the calcined clays shows better physical properties.
2. Among the three clays and alumina sources, pure calcined Neyveli clay and fine alumina form better mullite crystals with good physical properties.
3. The mullite prepared from Udayarpalayam clay shows imperfect morphology, with the presence of higher amount of secondary mullite crystals than the primary crystals, due to the presence of impurities.
4. The mullite prepared using boehmite exhibits good mullite microstructure with high aspect ratio, due to purity, fine particle size and homogeneous mixing with clays. However the high water loss in boehmite creates surface cracks resulting in poor strength.

References

- [1] H. Schneider, Thermal expansion of mullite, *J. Am. Ceram. Soc.* 73 (1990) 2073–2076.
- [2] M. Bartsch, B. Saruhan, M. Schmucker, H. Schneider, Novel low-temperature processing route of dense mullite ceramics by reaction sintering of amorphous SiO₂-coated γ -alumina particle nanocomposites, *J. Am. Ceram. Soc.* 74 (1999) 2448–2452.
- [3] M.D. Sacks, H. Lee, J.A. Pask, A review of powder preparation methods and densification procedures for fabricating high density mullite, in: S. Somiya, R.F. Davis, J.A. Pask (Eds.) *Ceramic Transaction, Vol. 6, Mullite and Mullite Composites.*, Am. Ceram. Soc., Westerville, OH, pp. 167–208.
- [4] K. Okada, N. Otsuka, S. Somiya, Review of mullite synthesis routes in Japan, *Am. Ceram. Soc. Bull.* 70 (1991) 1633–1640.
- [5] D. Amutharani, F.D. Gnanam, Low temperature pressure less sintering of sol-gel derived mullite, *Mater. Sci. Eng. A264* (1999) 254–261.
- [6] W.E. Lee, W.M. Rainforth, *Ceramic Microstructures, Property Control by Processing*, Chapman and Hall, London, UK, 1994, pp. 299–311.
- [7] M.A. Sainz, F.J. Serrano, J.M. Amigo, J. Bastida, A. Caballero, XRD micro structural analysis of mullite obtained from kaolinite-alumina mixtures, *J. Eur. Ceram. Soc.* 20 (2000) 403–412.
- [8] J. Temuujin, K.J.D. Mackenzie, M. Schemuker, H. Schneider, J. McManus, S. Wimperies, Phase evolution in mechanically treated mixtures of kaolinite and alumina hydrates (gibbsite and boehmite), *J. Eur. Ceram. Soc.* 20 (2000) 413–421.
- [9] H.R. Rezaie, W.H. Rainforth, W.E. Lee, Mullite evolution in

- ceramics derived from kaolinite, kaolinite with added α -alumina and sol-gel precursors, *Trans. Br. Ceram. Soc.* 96 (1997) 181–187.
- [10] G.W. Brindley, M. Nakahira, The kaolinite–mullite reaction series, I, II, III, *J. Am. Ceram. Soc.* 42 (1959) 311–324.
- [11] S.M. Johnson, J.A. Pask, J.S. Moya, Influence of impurities on high temperature reactions of kaolinite, *J. Am. Ceram. Soc.* 65 (1982) 31–35.
- [12] H. Schneider, K. Okada, J. Pask, in: K. Okada (Ed.), *Mullite and Mullite Ceramics*, John Wiley and Sons, Chichester, UK, 1994, pp. 105–108.
- [13] V. Viswabaskaran, M. Balasubramanian F.D. Gnanam, Mullitisation behaviour of three Indian clays, *Ceram. Int.* 28 (2002) 557–564.
- [14] V. Viswabaskaran, M. Balasubramanian F.D. Gnanam, Characterisation of aluminous clays from Tamilnadu, *Trans. Ind. Ceram. Soc.* (in press).
- [15] A.K. Charkborthy, D.K. Ghosh, Reexamination of the kaolinite to mullite reaction series, *J. Am. Ceram. Soc.* 61 (1978) 170–173.
- [16] S.P. Chaudhuri, A review on the kaolinite–mullite transformation, *Trans. Ind. Ceram. Soc.* XXXVI (1977) 71–80.
- [17] R.W. Grimshaw. *The Chemistry and Physics of Clays and Allied Materials*, Ernest Benn Ltd, London, 1971, pp. 525–527.
- [18] M. Sathyakumar, PhD thesis, Anna University, Chennai, India, 2000.
- [19] K.S. Mazdiyasi, L.M. Brown, Synthesis and mechanical properties of stoichiometric aluminium silicate (mullite), *J. Am. Ceram. Soc.* 55 (1972) 548–552.
- [20] K.C. Liu, G. Thomas, Time–temperature–transformation curves for kaolinite– α -alumina, *J. Am. Ceram. Soc.* 77 (1994) 545–552.
- [21] J.F. Klug, S. Prochazka, R.H. Doremus, Alumina–silica phase diagram in the mullite region, *J. Am. Ceram. Soc.* 70 (1987) 750–759.
- [22] K.K. Khandal, P.K. Gangopadhyay, T.C. Rao, Characterisation of three Indian clays, *Trans. Ind. Ceram. Soc.* 44 (1985) 82–88.